EARTHQUAKE ENGINEERING AND STRUCTURAL DYNAMICS, VOL. 24, 395–409 (1995)

AN ENERGY APPROACH TO SLIDING OF SINGLE-SPAN SIMPLY SUPPORTED SLAB-ON-GIRDER STEEL HIGHWAY BRIDGES WITH DAMAGED BEARINGS

MURAT DICLELI

Structural Design Consultant, Morrison Hershfield Ltd, Ottawa, Canada

AND

MICHEL BRUNEAU*

Department of Civil Engineering, University of Ottawa, Ottawa, Ontario, Canada K1N 6N5

SUMMARY

This paper investigates the non-linear inelastic seismic response of existing single-span simply supported bridges having bearings which can remain stable and slide after their anchor bolts are ruptured. A simplified equivalent model is developed for the inelastic analysis of these single-span simply supported bridges. Non-linear inelastic time-history analyses are conducted for various acceleration inputs. It is found that narrower bridges with longer spans may have considerable sliding displacements and fall off their supports if adequate seat width is not provided. It is also found that for the same ratio of friction coefficient to peak ground acceleration, the sliding displacement of a structural system is linearly proportional to the amplitude of the peak ground acceleration beyond a certain threshold value. This is also demonstrated analytically from an energy approach point of view. The distribution of the energy content of an earthquake, which is related to its velocity time history, can be an indication of the propensity of an earthquake to cause high sliding displacements. Ground motions with high frequency content or high A_p/V_p ratio may produce smaller sliding displacements than ground motions with relatively lower A_p/V_p ratios.

1. INTRODUCTION

The bearings which support the steel superstructure of single-span simply supported slab-on-girder bridges commonly used throughout the North American highway system, appear to be their weakest link of structural resistance to seismic loads. There exist many short to medium span old steel bridges supported by sliding bearings never designed for seismic resistance and thus vulnerable to earthquakes. The loss of lateral support due to bearings damage has been responsible for several bridge collapses in past earthquakes, notably during the 1971 San Fernando California, 1976 Guatemala, and 1980 Eureka earthquakes.[1] Even minor earthquakes have caused failure of anchor bolts, keeper bar bolts and welds in bridge bearings.[1] For many types of low-profile stable bearings, when the anchor bolts at the fixed type of sliding bearings are severed, the deck is free to slide. When such a failure happens, frictional forces will develop between the disconnected bridge components. This friction is, in some cases, the only possible 'second line of defense'.

In multi-span simply supported bridges, it is recognized that disconnected bridge components can be a most severe seismic hazard, and past research has investigated the effectiveness of, and demonstrated the need for, longitudinal restrainer ties at the expansion joints.[2,3] In fact, since they are most vulnerable to earthquakes, and because most bridge seismic-related research has been conducted in response to on-site failures during earthquakes, multi-span simply supported bridges have been extensively studied, particularly reinforced concrete ones. Analytical case studies on the seismic response of such bridges, considering their

*Associate Professor.

CCC 0098–8847/95/030395–15

Received 10 August 1993
Revised 18 May 1994

sliding in the longitudinal direction, among many factors, have been performed by many researchers (References 2, 4 and 5, to name a few). Some of their findings are equally applicable to steel and concrete bridges, such as, for example, the importance of providing shear keys in bridges.[6] However, seismic response problems germane to steel bridges, such as the need to restrain the displacement of unstable rocker bearings,[7] have generally received far less research attention.

Recent North American earthquakes have certainly demonstrated that steel bridges can also be vulnerable to earthquakes.[8-10] A sizable number of the existing steel bridges have never been designed to resist earthquakes, particularly in eastern North America, and a seismic retrofit of all these existing steel bridges is clearly prohibitive. Fortunately, if the aforementioned 'second line of defense' provided by frictional forces at the supports could be proven effective and sufficient to allow single-span simply supported steel bridges to resist small to moderate earthquakes, considerable savings are possible.

For seismic excitation in the longitudinal direction, when the friction resistance at the disconnected parts of single-span simply supported steel bridges is exceeded, collision of the deck with the abutment walls may occur repeatedly. Since there are abutment walls at each end of the bridge, the movement of the deck in the longitudinal direction is restricted by the width of the seat gap or expansion joint which is generally no more than 4–5 cm for the span ranges considered herein. Hence, in this direction, without concurrent severe abutment failures, the bridge is well constrained and the risk of failure is generally low.

For seismic excitation in the transverse direction, when the friction forces at the disconnected parts of single-span simply supported steel bridges are exceeded, the bridge deck slides, and may fall off its support under the following conditions: (i) The abutment's edge fails locally when the bearings slide to a point near the edge where insufficient bearing resistance can be provided to resist the normal reaction forces due to gravity loading. This could be either due to a reduction of bearing surface increasing the effective stresses to exceed the material's capacities, or, by the absence of adequate detailing to account for this shift in load application point. (ii) Sliding displacements exceed the distance between the bearing centreline and the support edge. Should this happen, the portion of the gravity load previously supported by the exterior girder is transferred to the nearest interior girder by cantilever action of the slab. If the slab does not have enough strength to resist this additional load, the exterior portion of the bridge deck could be severely damaged and make the bridge unusable. Therefore, sliding in the transverse direction seems critical and is studied in this paper from an energy approach point of view.

For the purpose of this study, a non-linear time-history analysis capable of accounting for the non-linear response at the expansion joints, namely impact and friction, is conducted. The objective in performing this analysis is to find the maximum transverse sliding displacement at the bearings as a function of various earthquake intensities, friction coefficients, span length and span width, and to establish a relationship between the magnitude of sliding displacement and peak ground acceleration to friction coefficient ratio. Existing knowledge on the modelling techniques and non-linear behaviour of bridge components[2,6,7,11-13] is used throughout this research to generate new information applicable specifically to single-span simply supported slab-on-girder steel bridges.

2. PROPERTIES OF THE BRIDGES STUDIED AND OTHER ASSUMPTIONS

To investigate the seismic performance of existing steel bridges never designed to resist earthquakes, two and three lane bridges with spans of 20, 30, 40, 50 and 60 m have been designed in compliance with the 1961 edition of the American Association of State Highways Officials (AASHO) code,[14] which is judged to be representative of the design requirements in effect at the time most highway bridges were constructed in North America. The 2 and 3-lane bridges have, respectively, 8 and 12 m widths and girders spaced at 2 m intervals. As seen in Figure 1, the deck of these bridges is generally attached to one abutment by fixed bearings and on the other abutment it is supported by expansion bearings. The fixed type of sliding bearings is shown in Figure 2. The expansion type of bearing is nearly identical, but without the longitudinal stopper bars. The manner in which these bearings can slide following rupture of their anchor bolts is illustrated in Figures 3 and 4 for sliding in the longitudinal and transverse directions, respectively. A 1 m overhang is assumed on both sides of the decks for all the bridges. Reinforced concrete deck is 200 mm thick.

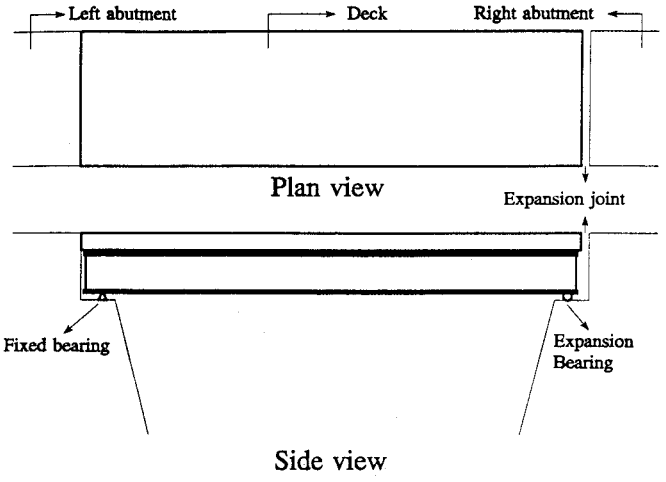

Figure 1. Typical single-span simply supported bridge

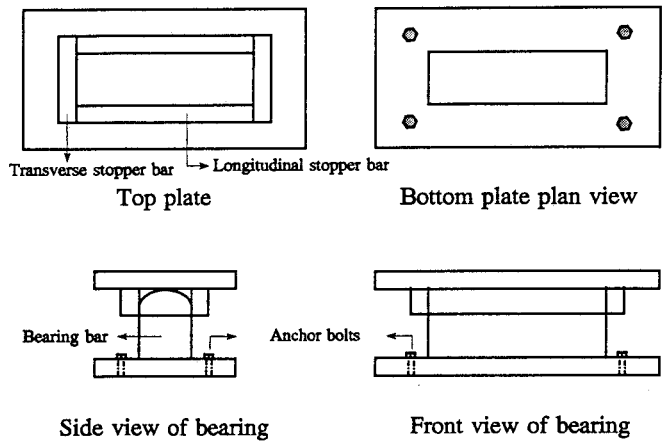

Figure 2. Typical fixed sliding bearing

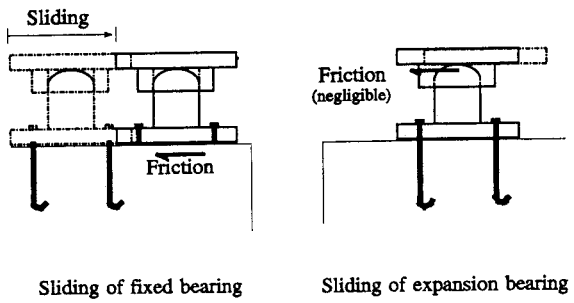

Figure 3. Sliding of bearings in longitudinal direction

Other important assumptions made for this study include the following.

(1) Only low-profile stable bearings are considered in this study. Although it might be possible to extend the findings to cases where girders sit directly on the abutments after the failure of unstable bearings, this has not been formally investigated herein.

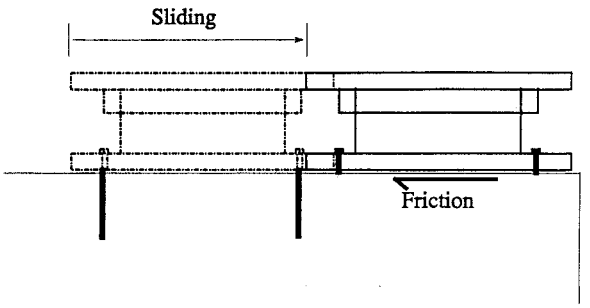

Figure 4. Sliding of bearings in transverse direction

(2) The friction coefficient is assumed constant throughout the sliding history.
(3) The effect of vertical ground accelerations on friction forces at the bearings has been neglected. The magnitude of the vertical reaction force on bearings undoubtedly vary due to vertical ground accelerations, and consequently, so does friction resistance throughout the earthquake. However, seismic vertical accelerations generally have a much higher frequency content than the corresponding horizontal ones, and it is reasonable to assume that the resulting fluctuations of frictional resistance will average themselves during any sliding excursion, simultaneously abating the significance of vertical accelerations.
(4) Only single-degree-of-freedom (SDOF) response was considered in this study. Analyses conducted by the authors have revealed that higher mode effects do not have a large impact on sliding.
(5) Skewed bridges have not been considered in this study. The higher seismic vulnerability of skewed bridges is well recognized, and the recent Northridge earthquake provided striking examples of poor seismic behaviour.[10] In these bridges, longitudinal and transverse seismic excitations can combine to produce excessive force and/or displacement demands at the various supports, a particular problem which depends in a complex manner on the bridge configuration, angle of skew, number of skewed supports and respective orientation of these various supports. Skewed bridges deserve a particular treatment which is obviously beyond the scope of work reported herein.
(6) Abutments and foundations deformations and/or damage as well as soil–structure interaction are beyond the scope of this study.

Other minor assumptions will be introduced when appropriate throughout this paper.

3. EARTHQUAKE LOADING

Ground motions can be characterized by the peak acceleration to peak velocity ratio, A_p/V_p, where A_p is expressed in units of the gravitational acceleration and V_p is expressed in meters per second.[15] Ground motions with very high-frequency content would produce high A_p/V_p ratios, whereas ground motions with intense long duration acceleration pulses would generally lead to low A_p/V_p ratios. The ground motions with highly irregular acceleration patterns result in intermediate A_p/V_p ratios.

Accordingly, four Western U.S.A. earthquake records having intermediate A_p/V_p ratios, all recorded on rock or stiff soil, and two Eastern Canada earthquake records having high A_p/V_p ratios, one on bedrock and another on alluvion deposit, are considered for the non-linear time-history analyses. The mean plus one standard deviation (MP1SD) spectrum of Western U.S.A. earthquakes[16] and spectra of Eastern Canada earthquakes are shown in Figure 5. The vertical axis in Figure 5 is, β, which is the ratio of the pseudo-spectral acceleration, S_a, to the peak ground acceleration A_p. Additionally, a record from the Erzincan earthquake, which has occurred in eastern Türkiye (Turkey), is also considered in one of the analyses due to its interesting acceleration time-history characteristics, which are: the concentration of nearly all input energy over a short

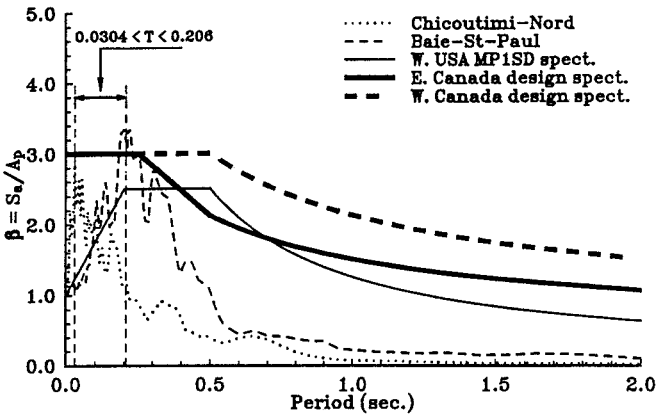

Figure 5. Elastic response spectra of Eastern Canada and western U.S.A. earthquakes for 5 per cent damping

Table I. Properties of the selected earthquakes

Site (1)	Location (2)	Date (3)	Component (4)	Magnitude (5)	Source distance (km) (6)	Soil type (7)	Max. acceleration ($\times g$) (8)
Imperial Valley	El Centro	1940	S00E (NS)	6·6	8	Stiff soil	0·348
Kern County	Taft	1952	S69E	7·6	56	Rock	0·179
San Fernando	Pacoima Dam	1971	S16E	6·6	8	Rock	1·170
Parkfield	Chaloma Shand. 2	1966	N65E	5·6	0·1	Stiff soil	0·480
Québec	Chicoutimi-Nord	1984	N18E	6·0	43	Rock	0·131
Québec	Baie-St-Paul	1982	S59E	6·0	91	Alluvium	0·174
Türkiye	Erzincan	1992	NS	6·9	7	Alluvium	0·500

time interval, its low A_p/V_p ratio, and the presence of three successive large acceleration pulses.[17] The properties of all the earthquake motions used in this study are shown in Table I.

4. NON-LINEAR INELASTIC MODELLING

4.1. Assumptions in modelling

The ultimate strength of bearings is obviously larger than their frictional resistance alone, i.e. a force larger than the bearing strength is required first to rupture actually the anchor bolts since bearing and friction are coexistent prior to the initiation of pure sliding, as illustrated in Figure 6. However, this aspect of behaviour is not included in the model nor is it accounted for by the computer program used. Instead, the bearings are assumed to be immediately damaged and their initial contribution is ignored. Since the peak of ultimate bearing resistance prior to anchor bolt failure, as illustrated in Figure 6, occurs only once and does not affect significantly the total amount of energy dissipated through sliding, refinements of the hysteresis models are unwarranted. Accordingly, a rigid-plastic hysteresis model is assumed to simulate the sliding of the bridge at the supports.

In the non-linear inelastic model, free rotation at both ends of the bridge is assumed. Although, some rotational resistance is produced by the longitudinal direction friction forces at the end of the bridge where fixed bearings are located as shown in Figure 7, results from elastic analyses showed that these rotationally induced longitudinal forces are extremely large and as much as five times the friction forces calculated using

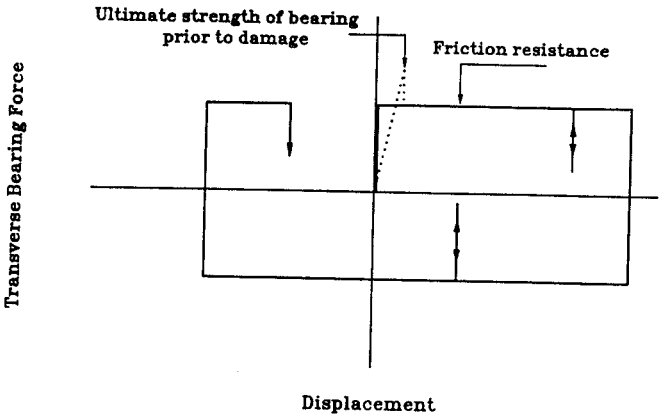

Figure 6. Bearing force vs. sliding displacement hysteresis models including and neglecting the ultimate bearing strength before damage occurs

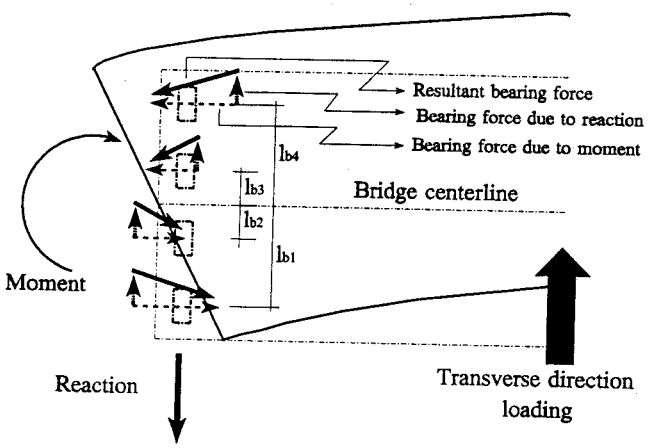

Figure 7. Bearing friction forces due to loading in transverse direction

a friction coefficient of 0·4. Results from elastic analyses also showed that the longitudinal displacements at the bearings due to free rotation at the support are very small, even for the wider bridges. Therefore, only a negligible amount of energy is dissipated when the bridge end rotates. Consequently, the assumptions made in modelling do not produce significant errors in simulating the behaviour of the actual system.

4.2. Description of the model

For the purpose of this study, a simplified equivalent model is used to simulate the non-linear behaviour of the actual structure using the program NEABS.[18] The deck of bridges considered in this study is composed of deep steel girders supporting a thick reinforced concrete slab. It acts as a very stiff element in its horizontal plane which has adequate strength reserve to resist seismic loads elastically, until the bearings are damaged. From the elastic analyses, it is found that the fundamental transverse direction mode of vibration of simply supported bridges is dominant. Therefore, the structure is idealized as a single-degree-of-freedom (SDOF) system which slides once the friction resistance is exceeded. It is customary to represent the mode shape of the real system by the following trigonometric function:

$$\Phi(x) = \sin \frac{\pi x}{L} \tag{1}$$

where L is the span length. Then, the generalized mass m^*, stiffness k^* and the effective force P_{eff} for the equivalent model are calculated as;[19]

$$m^* = \int_0^L \frac{m}{L}(\Phi(x))^2 \, dx = \int_0^L \frac{m}{L} \sin^2 \frac{\pi x}{L} \, dx = \frac{m}{2} \tag{2}$$

$$k^* = \int_0^L EI_D \left(\frac{d^2\Phi(x)}{dx^2}\right)^2 dx = \int_0^L EI_D \left(\frac{\pi^2}{L^2} \sin \frac{\pi x}{L}\right)^2 dx = \frac{\pi^4 EI_D}{2L^3} \tag{3}$$

$$P_{\text{eff}} = \ddot{u}_g \int_0^L \frac{m}{L} \Phi(x) \, dx = \ddot{u}_g \int_0^L \frac{m}{L} \sin \frac{\pi x}{L} \, dx = \frac{2m}{\pi} \ddot{u}_g \tag{4}$$

where m is the mass of the bridge, I_D is the moment of inertia of the bridge deck about a vertical axis and $\ddot{u}_g$ is the acceleration of the ground motion. Normally, when a SDOF system with a mass, m^*, is subjected to ground motion, the force acting on the system is customarily its mass times the ground acceleration, i.e. $m^*\ddot{u}_g$. However, note that for the simplified equivalent system considered herein, it is the effective force calculated above which acts on the system, not $m^*\ddot{u}_g$. Therefore, the ground acceleration history is corrected by an acceleration modification factor, AMF, as expressed below:

$$\text{AMF} = \frac{P_{\text{eff}}}{m^*\ddot{u}_g} = \frac{4}{\pi} \tag{5}$$

The idealized structure model and the actual system are illustrated in Figure 8. The bridge deck is modelled using a NEABS beam element with negligible flexural stiffness but with axial stiffness equal to k^*. An expansion joint element with a sliding elastic subelement is used for the model.

For a constant value of friction coefficient, the magnitude of Coulomb friction force is proportional to the reaction force, and therefore, sliding of the bridge is proportional to the ratio of the seismic force acting on the system to the reaction force. However, the seismic forces acting on the actual bridge and the simplified equivalent model are not identical. Accordingly, a modified vertical force, R^*, is also needed to represent the sum of the reaction forces on the bearings due to the weight of the bridge on the simplified equivalent system so that sliding occurs at the same time in both the equivalent and real systems. The ratio of R^* to the reaction force, R, on the real system, should be equal to the ratio of seismic force acting on the equivalent model to that acting on the real system, so that, sliding occurs at the same time in the equivalent system as it would occur in the real system. The seismic force acting on the equivalent model, before sliding, is expressed as

$$H^* = (\text{AMF } S_a)m^* = \frac{2}{\pi} m S_a \tag{6}$$

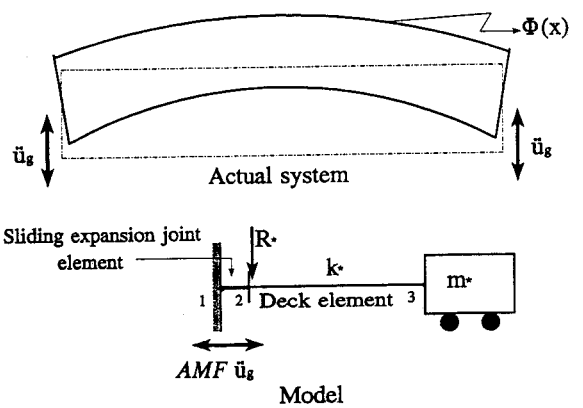

Figure 8. Actual system and simplified equivalent non-linear inelastic model

where S_a is the pseudo-acceleration of the structure before sliding. The total seismic force acting on the real system is expressed as

$$H = \frac{\mathscr{L}^2}{m^*} S_a = \frac{8}{\pi^2} m S_a \tag{7}$$

where $\mathscr{L}$ is the earthquake excitation factor. Then, the modified vertical force is defined as

$$R^* = \frac{H^*}{H} R = \frac{\pi}{4} R \tag{8}$$

This modified vertical force is applied on the beam node connected to the expansion joint element in the equivalent model. Finally, mass proportional damping and 5 percent damping are considered.

5. MINIMUM PEAK GROUND ACCELERATION REQUIRED FOR SLIDING

The sliding of the bridge in the transverse direction, after the bearings are damaged, may take place depending on the intensity of the earthquake. For sliding to occur, the total transverse seismic load, H, as expressed by equation (7), must be at least equal to the sliding resistance force, F_s, described for single-span simply supported bridges as

$$F_s = \mu_f m g \tag{9}$$

where μ_f is the coefficient of friction and g is the gravitational acceleration. Expressing the absolute spectral acceleration, S_a as $\beta \cdot A_p$, and using equations (7) and (9), the minimum value of peak ground acceleration required for sliding is expressed as

$$A_p = \frac{\pi^2}{8\beta} \mu_f g \tag{10}$$

The fundamental periods of the simply supported bridges considered here increase with span length, as mass increases and stiffness decreases. These periods fall in the small period range of the response spectra, and vary from 0·0304 to 0·206 s. As seen in Figure 5, in that portion of the response spectra, β increases as the period increases. Thus, the minimum peak ground acceleration required for sliding decreases as the span length increases for the ranges of spans considered (i.e. 20–60 m).

6. SLIDING OF BRIDGES IN THE TRANSVERSE DIRECTION

The previously described bridges (see Section 2) are analysed for five different coefficients of friction using the four Western U.S.A. and two Eastern Canada earthquakes listed in Table I. Sliding displacements at the support of 2-lane and 3-lane simply supported bridges are plotted as a function of span length for various friction coefficient to peak ground acceleration ratios, μ_f/A_p (A_p is expressed as a percentage of g), in Figures 9–12. In these figures, the vertical axis is the support sliding displacement in mm per unit peak ground acceleration and the horizontal axis is the span length. A total of 300 cases are analysed using the program NEABS to express visually the relationship between sliding displacement and peak ground acceleration, friction coefficient as well as the span length for various earthquakes. In the analyses, the peak ground acceleration of all the earthquakes, are scaled to 0·4 g, while the coefficient of friction is varied between 0·1 and 0·8. Additionally, keeping the μ_f/A_p ratio constant, but changing the magnitude of the peak ground acceleration, 60 new cases are also analysed using the same six earthquakes, two different A_p and five bridges of different span length, to obtain a relationship between the magnitude of the peak ground acceleration and sliding displacement. It is found that for the same μ_f/A_p ratio, the sliding displacement is linearly proportional to the amplitude of the peak ground acceleration. This dependency can be explained by an energy formulation of the sliding problem.

7. ENERGY APPROACH TO SLIDING

Consider that the previously defined equivalent SDOF system shown in Figure 8 is subjected to a ground motion. The total and relative displacements, u_t and u, of the mass of the system are expressed by the following equations;

$$u_t = u_g + u_s + u_e \tag{11}$$

$$u = u_s + u_e \tag{12}$$

where u_g is the ground displacement, and u_s and u_e are, respectively, the sliding and elastic displacements of the mass. Identical and valid expressions can be obtained for velocities and accelerations simply by first and second time derivatives of the above equations. Considering the equilibrium of the mass of the system just before sliding, the equation of motion is expressed as

$$m^* \ddot{u}_t + c^* \dot{u}_e + k^* u_e = 0 \tag{13}$$

where c^* is the viscous damping coefficient. During sliding, the sum of damping and elastic restoring forces is constant and equal to the friction resistance F_s. Knowing this and expressing the total acceleration as the sum of the relative and ground acceleration, the above equation is rewritten as

$$m^* \ddot{u} + F_s = -m^* \ddot{u}_g \tag{14}$$

The friction resistance for the equivalent SDOF system is expressed as

$$F_s = \mu_f R^* \tag{15}$$

Substitute the above equation into equation (14) and integrate with respect to the relative displacement:

$$\int m^* \ddot{u}\, du + \int \mu_f R^* du = -\int m^* \ddot{u}_g\, du \tag{16}$$

The first term on the left-hand side of the above equation is the relative kinetic energy of the system expressed as

$$E_{Rk} = \int m^* \ddot{u}\, du = \int m^* \frac{d\dot{u}}{dt}\, du = \int m^* \dot{u}\, d\dot{u} = m^* \frac{\dot{u}^2}{2} \tag{17}$$

During sliding, for an undamped system, elastic displacement stays as it was just before sliding and therefore the incremental change in relative displacement, du, is actually equal to the incremental change in sliding displacement du_s. Consequently, the second term on the left-hand side of equation (16) is the energy dissipated by friction and expressed in the following form:

$$E_f = \int \mu_f R^*\, du_s = \mu_f R^* u_s \tag{18}$$

The term on the right-hand side of equation (16) is the relative input energy, E_{Ri}, of the system. This input energy represents the work done by the seismic force $m^* \ddot{u}_g$, on the equivalent SDOF system.

Using these energy terms, the energy dissipated by friction is expressed as

$$E_f = E_{Ri} - E_{Rk} \tag{19}$$

Assume that the friction coefficient and the ground motion are scaled by a factor r_1 and due to this, the relative or sliding displacement increases r_2 times. The new scaled energy terms E_f^+, E_{Ri}^+ and E_{Rk}^+, respectively, for friction, relative input and relative kinetic energy are expressed as follows:

$$E_f^+ = (r_1 \mu_f) R^* (r_2\, u_s) = r_1 r_2 \mu_f R^* u_s = r_1 r_2 E_f \tag{20}$$

$$E_{Ri}^+ = -\int m^* (r_1 \ddot{u}_g)(r_2\, du) = -r_1 r_2 \int m^* \ddot{u}_g\, du = r_1 r_2\, E_{Ri} \tag{21}$$

$$E_{Rk}^+ = m^* \frac{(r_2 \dot{u})^2}{2} = r_2^2\, m^* \frac{\dot{u}^2}{2} = r_2^2 E_{Rk} \tag{22}$$

The new friction energy is equal to the new relative input energy minus the new relative kinetic energy, i.e.

$$r_1 r_2 E_f = r_1 r_2 E_{Ri} - r_2^2 E_{Rk} \tag{23}$$

Simplifying the above equation,

$$E_f = E_{Ri} - \frac{r_2}{r_1} E_{Rk} \tag{24}$$

Comparing the above equation with equation (19), for energy equilibrium, r_2 should be equal to r_1. In other words, when the friction coefficient and the ground motion are scaled by a factor r_1, the sliding displacement increases by the same factor. This also proves that, for the same ratio of friction coefficient to peak ground acceleration, the sliding displacement of a structural system is linearly proportional to the magnitude of the peak ground acceleration. The small levels of damping present in steel bridges do not affect meaningfully the above results.

For example, a 60 m span, 2 lane simply supported bridge with $\mu_f = 0{\cdot}1$ is subjected to the S69E component of the 1952 Taft earthquake scaled to $A_p = 0{\cdot}2\ g$. The μ_f/A_p ratio is 0·1 divided by 0·2, i.e. 0·5, and the sliding displacement obtained from non-linear inelastic time-history analysis is 63 mm. If the same bridge, but with $\mu_f = 0{\cdot}2$, is subjected to the same earthquake now scaled to $A_p = 0{\cdot}4\ g$, the same μ_f/A_p ratio of 0·5 is obtained. However, the sliding displacement in this second case is calculated to be 125 mm, almost twice the displacement obtained for the smaller peak ground acceleration. In both cases, the resulting u_s/A_p is 315 as predicted by the above proposed normalization method. It is noteworthy that in the above analysis, a 125 mm sliding displacement is obtained instead of the expected 126 mm displacement. This is primarily due to the negligible effect of 5 per cent damping included in the analysis.

8. INTERPRETATION OF THE RESULTS

The transverse direction sliding displacements of 2- and 3-lanes bridges for Western U.S.A. earthquakes are depicted, respectively, in Figures 9 and 10. These sliding displacements are obtained by averaging the results obtained using the four Western U.S.A. earthquakes. It is observed that the sliding displacement increases for increasing span length and decreasing μ_f/A_p ratio.

The fundamental periods of the bridges fall in a part of the response spectra of the earthquake records shown in Figure 5. In that part of the spectra the amplitude increases with period. For the range of spans considered, bridges with longer span have larger periods; therefore, larger forces are applied on the bridges with longer span. This subsequently results in a higher amount of energy to be dissipated by friction and

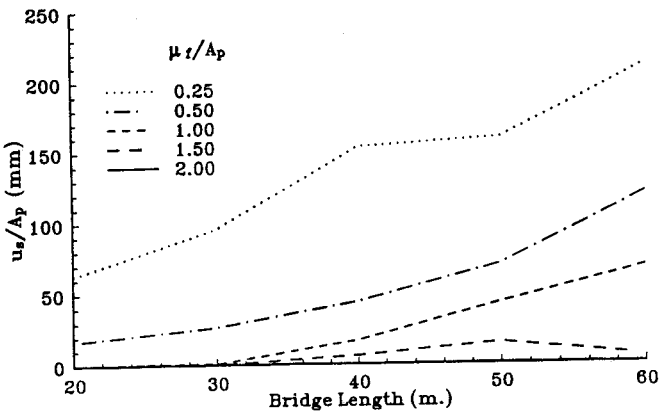

Figure 9. Transverse sliding displacement per peak ground acceleration (% g) of 2-lane bridges for various friction coefficient to peak ground acceleration ratios (average of Western U.S.A. earthquakes)

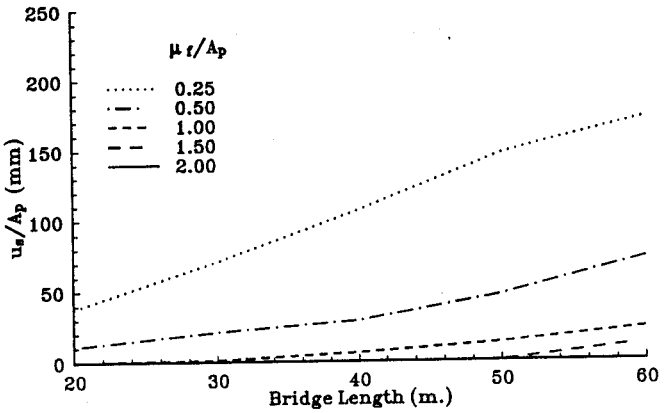

Figure 10. Transverse sliding displacement per peak ground acceleration (% g) of 3-lane bridges for various friction coefficient to peak ground acceleration ratios (average of Western U.S.A. earthquakes)

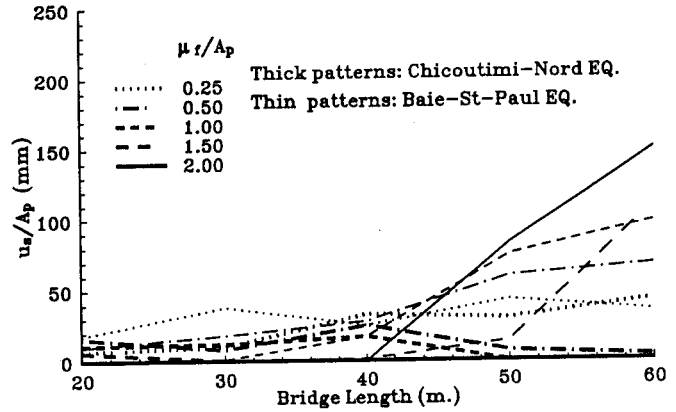

Figure 11. Transverse sliding displacement per peak ground acceleration (% g) of 2-lane bridges for various friction coefficient to peak ground acceleration ratios (Eastern Canada earthquakes)

consequently larger sliding displacements. Wider bridges have even smaller periods. Therefore, the attracted seismic forces are smaller than those for narrower bridges of the same length. Accordingly, sliding displacements of 3-lane bridges are smaller than those of 2-lane bridges as seen in Figures 9 and 10.

Figures 11 and 12 are, respectively, for the transverse sliding displacements of 2- and 3-lanes bridges for Eastern Canada earthquakes. Almost the same trend as for Western U.S.A. earthquakes is observed in the case of Baie-St-Paul earthquake. However, in the case of Chicoutimi-Nord earthquake, sliding displacements start decreasing for bridges of 50 m span and longer ($T_1 > 0.20$ s). As observed from the earthquake spectrum of Figure 5, for structures with fundamental periods longer than 0.2 s, the force applied on the structure decreases; hence the sliding displacement decreases.

9. EFFECT OF A_P/V_P RATIO OF EARTHQUAKES ON SLIDING DISPLACEMENTS

Ground motions are characterized by their A_P/V_P ratio. In this section the effect of this ratio on the magnitude of sliding displacement is investigated. Sliding displacement time history of a 2-lane, 60 m bridge is conducted using two different earthquakes: the 1940 El Centro S00E component and 1992 Erzincan, Türkiye NS component. The El Centro earthquake has highly irregular acceleration patterns, i.e. a mixture

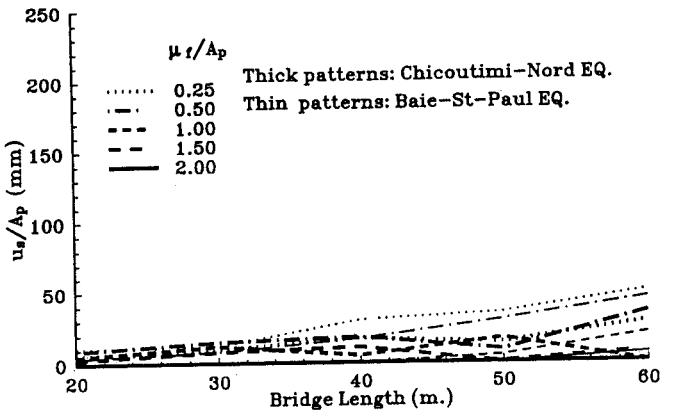

Figure 12. Transverse sliding displacement per peak ground acceleration (% g) of 3-lane bridges for various friction coefficient to peak ground acceleration ratios (Eastern Canada earthquakes)

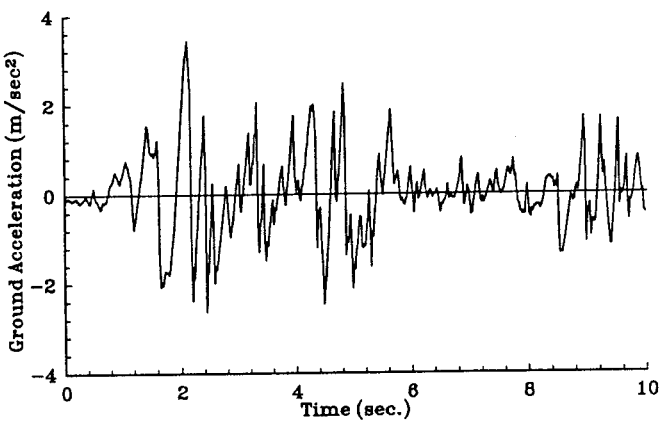

Figure 13. Ground acceleration time history of El Centro S00E earthquake, first 10 s

of short and medium duration pulses, and therefore has an intermediate A_p/V_p ratio, whereas the Erzincan earthquake has intense long duration acceleration pulses which results in a low A_p/V_p ratio. The peak accelerations of both earthquakes are scaled to 0·40g. The full acceleration records of both earthquakes are used in the analyses, but the maximum sliding displacements occurred within the first 10 s of both earthquakes. Therefore, only the first 10 s of the acceleration records and the sliding displacement histories are plotted in Figures 13 and 14 for the El Centro earthquake, and in Figures 15 and 16 for the Erzincan earthquake. The maximum sliding displacement obtained from the El Centro earthquake is 54 mm and it is 192 mm in the case of Erzincan earthquake. As seen in Figure 13, the El Centro earthquake contains generally high-frequency, irregular acceleration pulses, which load and unload the structure in short time periods. Therefore, once the structure starts to slide, this sliding motion cannot be sustained for a long time because the force applied on the system remains above the threshold of friction only for a short duration. Accordingly, in Figure 14, there is an irregularly increasing and decreasing sliding displacement plot, i.e. following a biased movement in a sliding displacement as a result of a relatively longer duration pulse, the structure undergoes small sliding displacements back and forth. On the contrary, as observed in Figure 15, the Erzincan earthquake contains pulses of long duration. Therefore, once the structure starts to slide, the motion can be sustained for a longer time, since the force applied on the system remains above the threshold

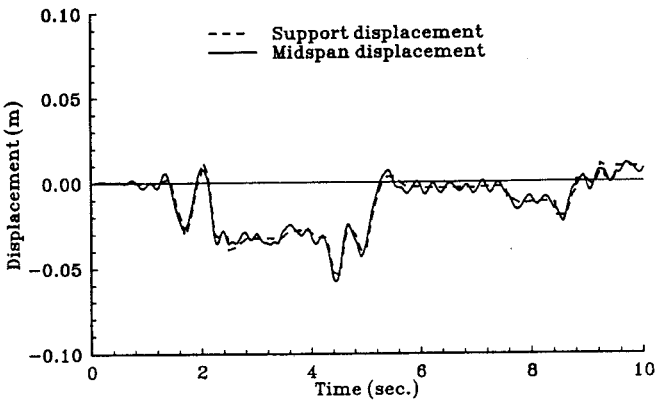

Figure 14. Support sliding time history of 2-lane 60 m simply supported bridge (El Centro S00E component $A_p = 0{\cdot}4\,g$)

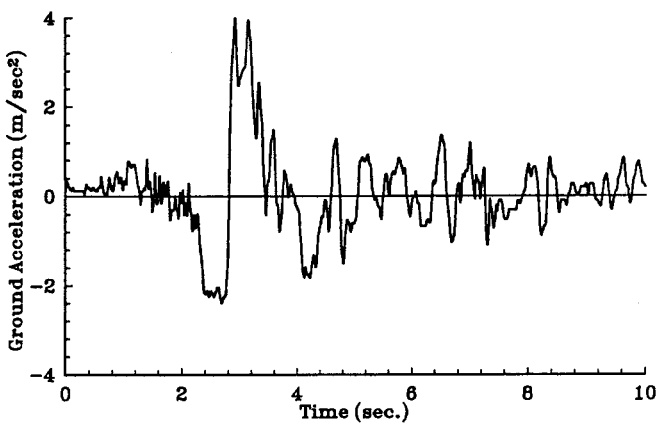

Figure 15. Ground acceleration time history of Erzincan, Türkiye, earthquake, first 10 s

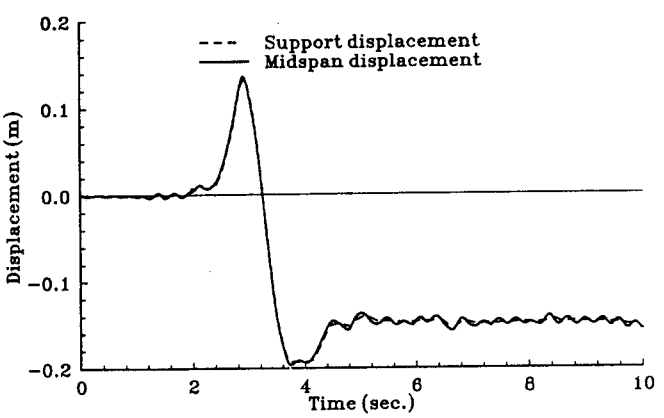

Figure 16. Support sliding time history of 2-lane 60 m simply supported bridge (Erzincan earthquake, NS component $A_p = 0{\cdot}4\,g$)

of friction for a long duration. Therefore, in Figure 16, a smoothly increasing sliding displacement is observed. Note that Figures 14 and 16 have different displacement scale and, as such, should not be misinterpreted.

Additionally, the sliding displacements obtained for the same bridge from the two Eastern Canada earthquakes used in this paper, are compared with those obtained from the El Centro and Erzincan earthquakes. These Eastern Canada earthquakes contain very high-frequency acceleration pulses, thus very high A_p/V_p ratios. As expected, the sliding displacements obtained from these earthquakes are not considerable and much less than the displacements calculated above, being 17 and 14 mm for Chicoutimi-Nord and Baie-St-Paul earthquake records respectively, when peak ground accelerations are consistently scaled to $0{\cdot}4g$.

These case studies confirm that distribution of the energy content of the earthquake, which is related to its velocity time history, can be an indication of the propensity of an earthquake to cause high sliding displacements. For earthquake records such as the Erzincan one, energy is concentrated over a short time period in three low-frequency, big acceleration pulses; hence, it produces high values of sliding displacements. However, for earthquake records like Chicoutimi-Nord and Baie-St-Paul, the energy is distributed over a longer time period in high-frequency pulses; hence, they are not as effective as the Erzincan earthquake. In other words, ground motions with high-frequency content or high A_p/V_p ratio produce very low sliding displacements, whereas ground motions with intense long duration acceleration pulses which have low A_p/V_p ratios can cause remarkable sliding displacements. Ground motions with highly irregular acceleration pulses and intermediate A_p/V_p ratios causes medium sliding displacements.

It is noteworthy that the effect of such sliding behaviour on the seismic resistance of continuous bridges having similar bearings capable to rupture in a stable manner has also been addressed elsewhere.[20] Although steel columns also affected seismic response, similar observations on the quite different vulnerability of bridges in Eastern and Western North America were made.

9. CONCLUSIONS

(a) For the same ratio of friction coefficient to peak ground acceleration, the sliding displacement of a structural system is linearly proportional to the amplitude of the peak ground acceleration.
(b) For the ranges of spans considered, sliding displacement increases with increasing span length and decreasing μ_f/A_p ratio.
(c) Sliding displacements of 3-lane bridges are smaller than those of 2-lane bridges. Nevertheless, the displacements are not considerable in both cases for the earthquakes and range of spans considered.
(d) The distribution of the energy content of an earthquake, which is related to its velocity time history, can be an indication of the propensity of an earthquake to cause high sliding displacements. This relationship between sliding and seismic energy has been analytically demonstrated in this paper. Ground motions with high-frequency content or high A_p/V_p ratio produce very small sliding displacements, whereas ground motions with intense long duration acceleration pulses or low A_p/V_p ratios can cause remarkable sliding displacements. Ground motions with highly irregular acceleration pulses which have intermediate A_p/V_p ratios produce medium sliding displacements. Accordingly, bridges in Western North America may potentially be subjected to higher sliding displacements than those in Eastern North America.

ACKNOWLEDGEMENTS

Financial assistance provided by the Natural Sciences and Engineering Research Council of Canada is gratefully acknowledged. The findings and recommendations in this paper, however, are those of the writers and not necessarily those of the sponsor.

REFERENCES

1. US Department of Transportation, *Seismic Design and Retrofit Manual for Highway Bridges*, Federal Highway Administration FHWA-IP-87-6, 1987.

2. W. S. Tseng and J. Penzien, 'Analytical investigations of the seismic response of long multiple-span highway-bridges', *Report No. EERC 73-12* Earthquake Engineering Research Center, University of California, Berkeley, CA, 1973.
3. J. Penzien and M. Chen, 'Seismic response of highway bridges', *Proc. 1st US natl conf. earthquake engineering, Ann Arbor, Michigan,* 1975.
4. M. Chen and J. Penzien, 'Analytical investigations of the seismic response of short, single or multiple-span highway bridges', *Report No. EERC 75-4,* Earthquake Engineering Research Center, University of California, Berkeley, CA, 1975.
5. R. M. Zimmerman and R. D. Brittain, 'Seismic response of multi-span highway bridges', *Proc. 3rd Canadian conf. earthquake engineering,* Montreal, P.Q., 1981 pp. 1091–1120.
6. R. A. Imbsen, and J. Penzien, 'Evaluation of energy absorbing characteristic of highway bridges under seismic conditions', *Report No. EERC 86/17,* Earthquake Engineering Research Center, University of California, Berkeley, CA, 1986.
7. M. B. Douglas 'Experimental dynamic response investigations of existing highway bridges', *Proc. workshop on earthquake resistance of highway bridges,* 1979 pp. 497–523.
8. K. L. Benuska (ed), 'Loma Prieta earthquake reconnaissance report', *Earthquake spectra* **6**, Supplement 90-01 (1990).
9. A. A. Astaneh, *Proc. 1st US seminar on the seismic evaluation and retrofit of steel bridges,* 1993.
10. Earthquake Engineering Research Institute, *Northridge Earthquake January 17, 1994, Preliminary Reconnaissance Report,* Earthquake Engineering Research Institute, Oakland, CA, 1994.
11. K. Kawashima and J. Penzien, 'Correlative investigations on theoretical and experimental dynamic behavior of a model bridge structure', *Report No. EERC 76-26,* Earthquake Engineering Research Center, University of California, Berkeley, CA, 1976.
12. R. A. Imbsen and J. Penzien, 'Evaluation of analytical procedures used in bridge seismic design', *Proc. workshop on earthquake resistance of highway bridges,* 1979, pp. 468–496.
13. J. C. Wilson, 'Analysis of the observed seismic response of a highway bridge', *Earthquake eng. struct. dyn.* **14**, 339–354, (1986).
14. American Association of State Highway Officials, *Standard Specifications for Highway Bridges,* Washington, DC, 1961.
15. T. J. Zhu, A. C. Heidebrecht, and W. K. Tso, 'Effect of peak ground acceleration to velocity ratio on ductility demand of inelastic systems', *Earthquake eng. struct. dyn.* **16**, 63–79 (1988).
16. M. Dicleli, 'Inelastic spectral analysis of structural systems under seismic excitations', *M.Sc. Thesis,* Department of Civil Engineering, Middle East Technical University, Ankara, Turkey, 1989.
17. M. Saatcioglu, and M. Bruneau, 'Performance of structures during Erzincan earthquake', *Canad. j. civil eng.* **20**, 305–325 (1993).
18. J. Penzien, R. Imbsen, and W. D. Liu, '*NEABS, Nonlinear Earthquake Analysis of Bridge Systems*', University of California, Berkeley, CA, 1981.
19. R. W. Clough, and J. Penzien, *Dynamics of Structures,* McGraw-Hill, New York, 1975.
20. M. Dicleli and M. Bruneau, 'Seismic performance of slab-on-girder single span simply supported and continuous steel highway bridges', *ASCE j. struct. eng. submitted.*